(Received 6 October 2023, Accepted 15 December 2023, Scheduled 24 December 2023)

Conformal Flexible Omnidirectional Rectenna Array Designed for Application in IoT Smart Water Meters

Ruinan Fan, Junlin Mi, Jianwei Jing, Liping Yan, and Changjun Liu*

School of Electronics and Information Engineering, Sichuan University, Chengdu 610064, China

ABSTRACT: In this manuscript, we propose a conformal and flexible meander dipole rectenna array for omnidirectionally harvesting ambient RF power for application in Internet of Things (IoT) water meters. The array unit consists of an antenna for RF power harvesting and a Schottky diode for converting the harvested RF power into DC power. The impedance between the antenna and diode is directly conjugated and matched using a meander structure and coupling loop. Traditional matching networks introduce additional losses, while direct conjugate matching maximizes power transmission efficiency and reduces energy losses. The elimination of the matching network simplifies the design of the rectenna, reducing the number of components and the overall size and weight. The rectenna unit is suitable for low-power ambient energy harvesting and operates at 2.45 GHz. The measured RF to DC conversion efficiency of the rectenna unit reaches 50% at 0 dBm. The rectenna array is formed by connecting eight antenna units in parallel, and units are affixed to the four surfaces of the water meter case to achieve omnidirectional RF environmental power harvesting. The output DC power of the array can be up to 1.3 mW at 100 μw/cm^2 received power density. An energy management circuit (BQ25504) is designed to store, distribute, and manage the harvesting of RF power to power the IoT water meter efficiently. Measured results demonstrated that the proposed rectenna array exhibited excellent adaptability and application potential in IoT scenarios.

1. INTRODUCTION

The rapid advancement of Internet of Things (IoT) technology has garnered significant interest in wireless energy transfer (WPT) [1–8]. Presently, WPT finds extensive application in areas such as smart home, smart healthcare, and smart management [9, 10].

A water meter is indispensable to monitor users' water consumption in daily life. Smart water meters integrate water monitoring sensors with IoT and upload real-time data on users' water consumption, providing great convenience [11, 12]. However, smart water meter batteries are difficult to maintain in humid and complex working environments and have high cost to replace due to the large number of meters. Consequently, the study of smart water meters powered by WPT is of great significance.

Microwave wireless power transfer (MWPT) has significant advantages in far-field WPT [13, 14], which is more suitable for the applications of smart water meters. A rectenna is an important part of an MWPT system [15]. In order to obtain high RF to DC conversion efficiency [16, 17], a conventional rectenna needs an impedance-matching network to match the rectifying circuit with a standard antenna impedance of 50 Ω. However, this inevitably enlarges the size of the rectenna. Therefore, eliminating the matching network by directly conjugating the diode's impedance with the receiving antenna's impedance is more in line with the miniaturization requirements of IoT sensors [18, 19]. In [20], a high-efficiency rectifying off-center-fed-dipole (OCFD) antenna without an impedance-matching network was proposed. [21] presented a high-efficiency, miniaturized rectenna operating in a low power density environment at 2.45 GHz.

Rectennas made of conventional substrates are usually rigid. They cannot adapt to IoT devices with variable external shapes. However, rectennas based on flexible substrates are able to conform to complex structures. [22] proposed a flexible and lightweight textile-integrated rectangular antenna array for powering wearable electronic devices. [23] investigated the problem of center frequency shift due to flexible meander antenna and proposed a wavefront WPT flexible antenna with frequency self-reconfiguration based on an electronic textile antenna for battery-free sensor platforms.

This manuscript proposes a conformal and omnidirectional rectenna array for RF energy harvesting in low-power-density environments for smart water meter applications. Section 2 discusses the mechanism of eliminating impedance-matching networks. Section 3 describes a meander dipole antenna that can conjugately match the impedance of rectifying diodes. Section 4 describes the fabrication and measurement of the rectenna unit. Section 5 analyses the measures of the rectenna array. Section 6 describes the design of the BQ25504 energy management circuit to power the smart water meter successfully.

2. RECTENNA THEORY WITH THE ELIMINATION OF MATCHING NETWORKS

Rectennas are an essential part of an MWPT system. The RF-to-DC conversion efficiency of a rectenna is closely related to the efficiency of the RF transmission system. The trans-

* Corresponding authors: Changjun Liu (cjliu@ieee.org).

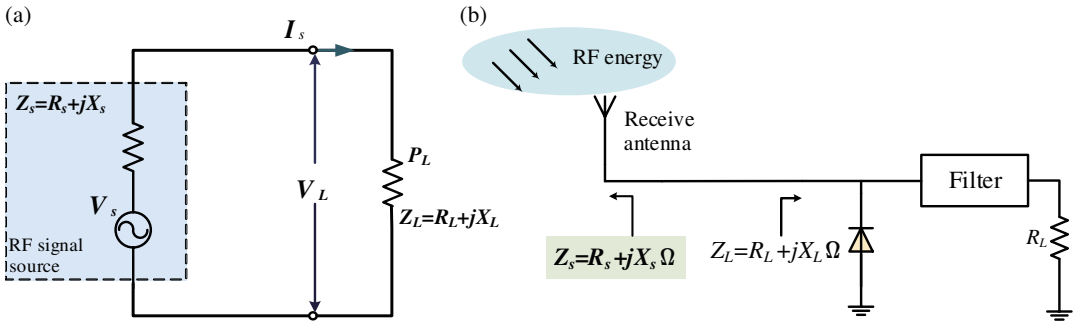

FIGURE 1. (a) RF transmission system. (b) Rectenna system structure without matching network.

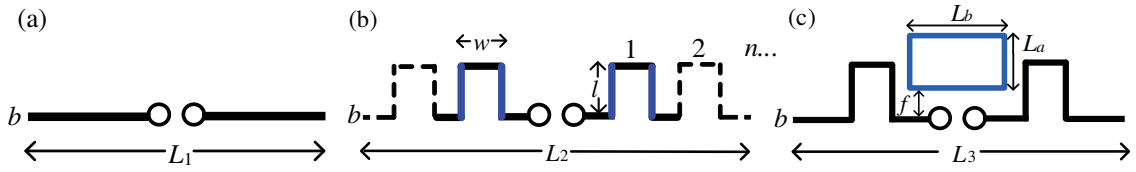

FIGURE 2. Dipole antenna. (a) Conventional structure. (b) Meander structure. (c) Coupling ring structure.

mission efficiency of an RF transmission system should be as high as possible for the load to obtain more power. Figure 1(a) shows that a facilitated RF transmission system contains a signal source with impedance $Z_S = R_S + jX_S$ and a load $Z_L = R_L + jX_L$. The effective voltage in the complex format of the signal source is $\dot{V}_s$. Then, the power P_L at the load Z_L is:

$$P_L = Re\left\{\dot{V}_L\dot{I}_s^*\right\} = Re\left\{Z_L\dot{I}_s\cdot\dot{I}_s^*\right\} = Re\left\{Z_L\left|\dot{I}_s\right|^2\right\}$$

$$= \left|\dot{I}_s\right|^2 R_L = \frac{R_L\left|\dot{V}_S\right|^2}{(R_s+R_L)^2+(X_s+X_L)^2} \quad (1)$$

where $\dot{I}_S$ is the effective current in the circuit.

To maximize P_L, it is necessary to satisfy $R_L = R_S$ and $X_L = -X_S$ simultaneously.

This indicates that the maximum transmission power is achieved when the load impedance Z_L is conjugately matched to the source impedance Z_S. Then, the power on the load is:

$$P_L = \frac{\left|\dot{V}_S\right|^2}{4R_L} \quad (2)$$

Therefore, the receiving antenna's impedance should conjugately match the rectifying circuit's impedance in an MWPT system to achieve maximum transmission efficiency. A conventional way is to design the receiving antenna's impedance as 50 Ω and introduce an impedance-matching network to transform the rectifying circuit's input impedance to 50 Ω.

However, the impedance-matching network will increase the size of the rectenna. Therefore, this manuscript adopts a rectenna design method to eliminate the impedance-matching network. The schematic of a rectenna without impedance-matching networks is shown in Figure 1(b). The input impedance of the antenna is directly conjugated with the impedance of the diode. The proposed rectenna design can maintain high conversion efficiency and reduce the rectenna size, eliminating the possible insertion loss caused by the impedance-matching network.

3. MEANDER DIPOLE RECTENNA DESIGN

A conventional half-wave dipole antenna consists of two straight metal conductors, as Figure 2(a) shows. The length of the antenna is about $1/2\lambda$. The input impedance of the dipole antenna is calculated by:

$$Z_{in} = 30\times[0.577+\ln(2\pi)-Ci(2\pi)+jSi(2\pi)] \quad (3)$$

According to formula (3), the input impedance of a conventional half-wave dipole antenna at 2.45 GHz is $(73+j42.5)\,\Omega$, and its length is about 61.2 mm.

Figure 2(b) shows meander structures, which allow the antenna to be more compact and increase its reactance. The input impedance of the dipole antenna with four meanders is shifted to $(31+j179)\,\Omega$ at 2.45 GHz.

However, due to the capacitive impedance of the diode, the meander dipole cannot accurately achieve a conjugate impedance match to it. Therefore, a coupling ring structure is introduced for better impedance matching with the diode, as shown in Figure 2(c). A coupling ring, which is a closed metal ring that mutually couples electromagnetic fields with the meander dipole antenna, is introduced. The antenna input impedance is tuned by varying the distance f between the coupling loop and the straight arm of the meander antenna. Meanwhile, the reactance of the antenna impedance is tuned almost independently by adjusting the length L_a or width L_b of the coupling loop.

The input impedance of the antenna with respect to f and L_b is simulated by the HFSS and is shown in Figure 3. It can be seen that the input resistance and reactance of the antenna

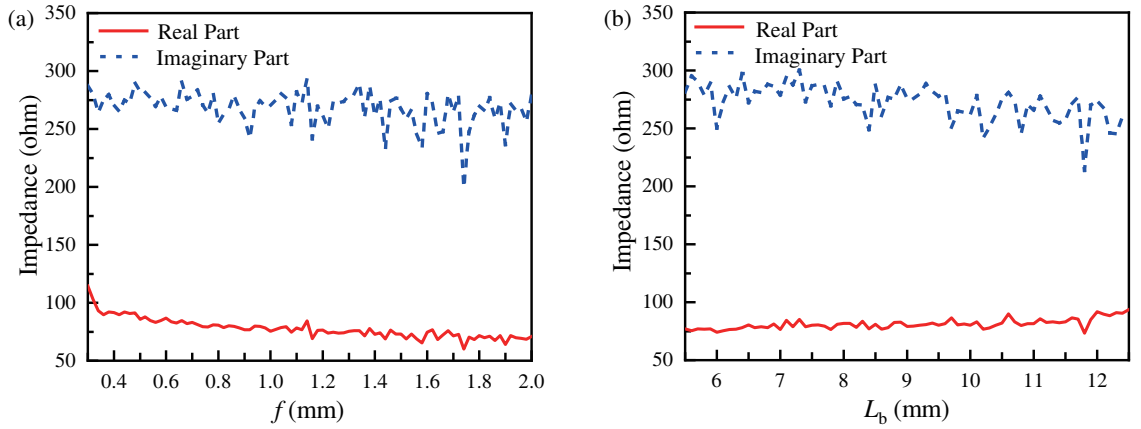

FIGURE 3. Input impedance with respect to the coupling loop parameters (a) f and (b) L_b.

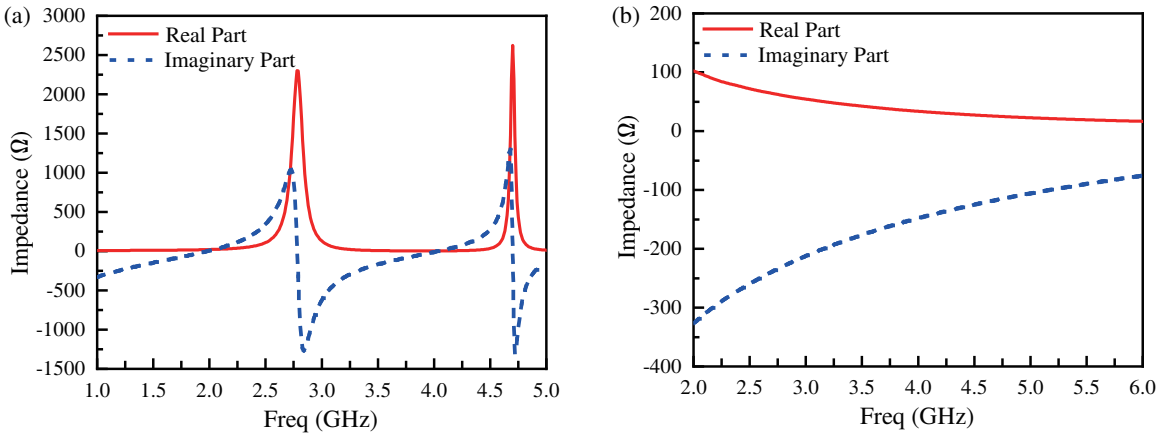

FIGURE 4. Impedances of the meander dipole antenna and diode. (a) HFSS simulation results of the antenna. (b) ADS simulation results of the diode.

decrease as f increases. As L_b increases, the input resistance of the antenna increases, and the antenna's reactance decreases.

The optimized simulation results are shown in Figure 4(a). At 2.45 GHz, the input impedance of the antenna is $(82.4 + j276.05)\,\Omega$, which is an ideal value that can be conjugately matched with the diode impedance.

4. FABRICATION AND MEASUREMENT OF THE RECTENNA

An SMS-7630 Schottky diode from Skyworks is selected to build the rectenna. Its main parameters are shown in Table 1. Due to its low on-state voltage, small zero-bias junction capacitance, and short transit time, it is suitable for low-power RF ambient energy harvesting for smart water meter applications.

The diode impedance is obtained from simulation based on the Advanced Design System (ADS) software with the nonlinear SPICE model. The results are shown in Figure 4(b) and Table 2. The impedance of the SMS-7630 diode is $(74.41 - j265.3)\,\Omega$ at 2.45 GHz, which can be conjugately matched with the proposed antenna.

The geometry and configuration of the proposed flexible meander dipole rectenna are shown in Figure 5. The top layer of the flexible substrate is polyimide with a thickness of 12.5 µm ($\varepsilon_r = 2.9$). The middle layer uses 18 µm thick copper as the radiation patch. The bottom layer uses 25 µm thick polyimide as the dielectric substrate. The dimension of the rectenna is 11 mm by 36 mm.

The SMS-7630 diode is placed at the center of the rectenna to convert the harvested RF power into DC power. Two inductors (820 nH) are placed at both ends of the meander line dipole antenna to block RF components.

The fabricated prototype rectenna is shown in Figure 6. The weight of a single flexible rectenna unit is only 0.12 g. The wires are soldered to the ends of the two inductors as DC outputs.

The proposed rectenna was measured in an anechoic chamber, as depicted in Figure 7. The RF signal is amplified by a power amplifier and transmitted by a standard horn antenna with a gain of 12.95 dB. A power meter (Mini-Circuit) connected to the 30 dB directional coupler was used to measure the transmitted power. The rectenna unit harvested energy at a distance of 1.3 m from the horn antenna (far field region). The

TABLE 1. Parameters of SMS-7630 diode.

V_{bi}/V	V_{br}/V	C_{j0}/pF	I_S/μA	R_S/Ω
0.18	2	0.14	5	20

TABLE 2. The input impedance of the meander line dipole antenna and SMS-7630 diode.

Component	Frequency/GHz	Impedance/Ω
meander line antenna antenna	2.45	$82.4 + j276.05$
SMS-7630	2.45	$74.41 - j265.3$

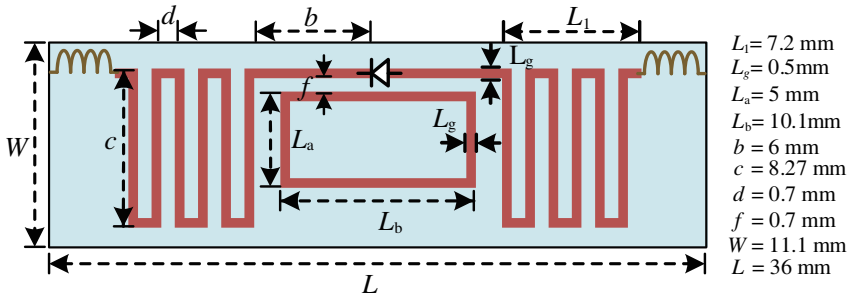

FIGURE 5. Geometry and configuration of the proposed rectenna.

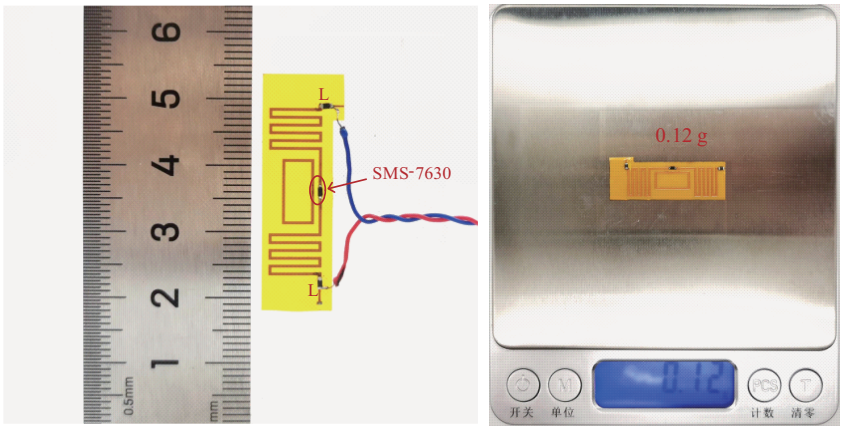

FIGURE 6. Fabricated prototype rectenna.

output DC voltage (V_{dc}) was measured by a multimeter, and the output DC power was calculated from $P_{out} = V_{dc}^2/R_{load}$.

The received power P_r of the rectenna can be calculated by multiplying the effective area of the antenna A_e with the average power density S_{avg} at the surface of the rectenna:

$$P_r = A_e S_{avg} = \frac{G_t P_t A_e}{4\pi R^2} \tag{4}$$

where P_t is the transmit power measured by the power meter, G_t the dimensionless transmit antenna's gain, and R the distance between the transmitting and receiving antenna. We approximate the effective area A_e by the actual physical area of the rectenna. The value of A_e is 7.7 cm^2.

The RF-to-DC conversion efficiency is:

$$\eta = \frac{V_{dc}^2}{P_r \times R_{load}} \times 100\% \tag{5}$$

The relationship between the load and the conversion efficiency is shown in Figure 8(a) when the received power of the rectenna is 7.4 dBm at 2.45 GHz. It shows that with the increase of the load, conversion efficiency first rises and then decreases. When the load is 300 Ω, the measured maximum conversion efficiency is reached, the output DC voltage is 1.08 V, the output DC power is 3.89 mW, and the conversion efficiency is 64.19%.

The rectenna conversion efficiencies versus the received power at 2.45 GHz with a DC load of 300 Ω are shown in Figure 8(b). The results show that as the input power P_r increases, the conversion efficiency increases first, reaches the peak, and then drops. The measured highest conversion efficiency of 64.65% is achieved at 6.8 dBm input power, and the output DC voltage is 0.966 V. The measured conversion efficiency is greater than 50% from −1 to 10 dBm.

Comparison between the simulated and measured conversion efficiencies of the rectenna is shown in Figure 8. The simulation and measurement results remain relatively consistent.

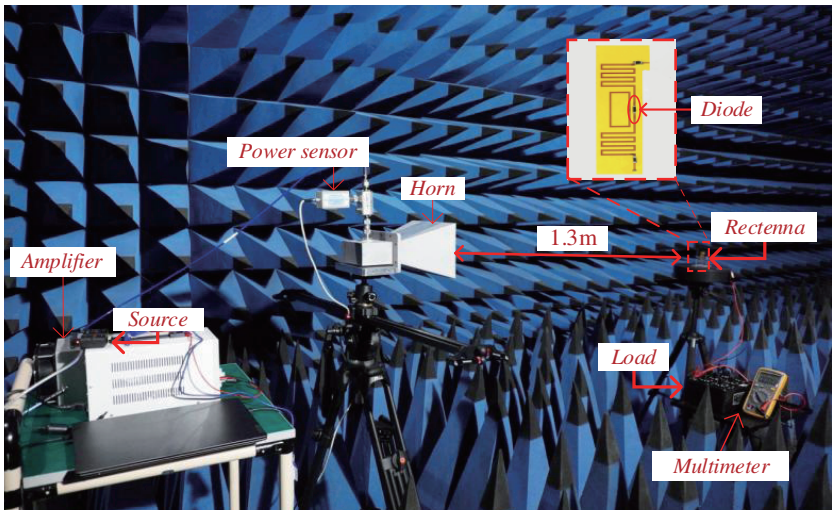

FIGURE 7. The test system of the rectenna unit.

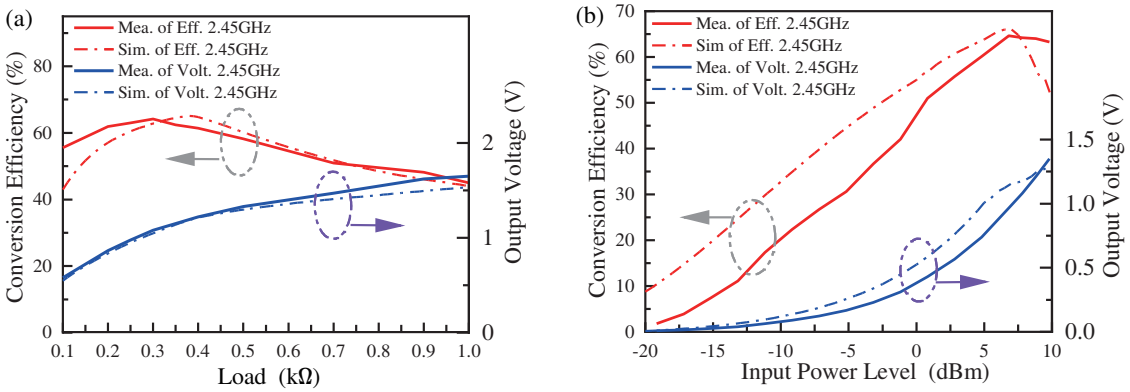

FIGURE 8. Rectenna unit simulation and measurement. (a) Conversion efficiency with various loads. (b) Conversion efficiency with different input power levels.

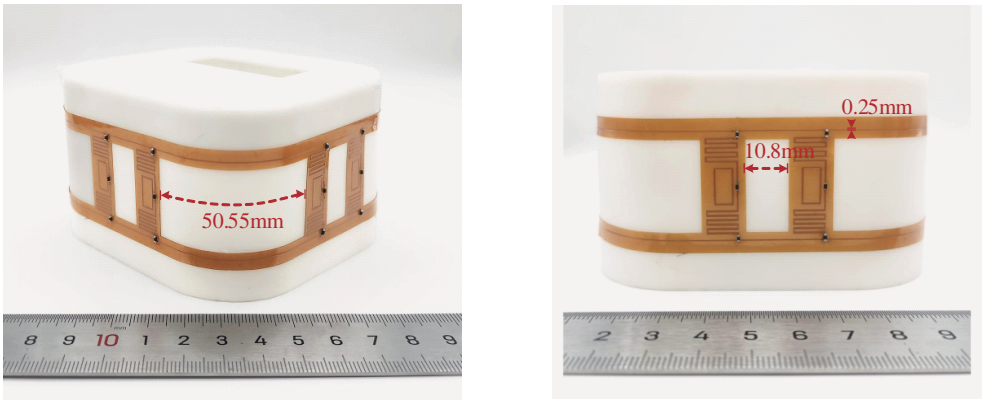

FIGURE 9. Rectenna array on the water meter case.

5. FABRICATION AND MEASUREMENT OF RECTENNA ARRAY

Concerning the practical implementation of the smart water meters, the rectenna array must be omnidirectional. As depicted in Figure 9, the proposed flexible rectenna array conforms to the water meter's outer surface and consists of eight parallel connected flexible rectenna units. Two units are placed on one side of the water meter case, while another two units are placed on the other side. The spacing between the two units is 10.8 mm on the same side and 50.55 mm on the different sides. 0.25-

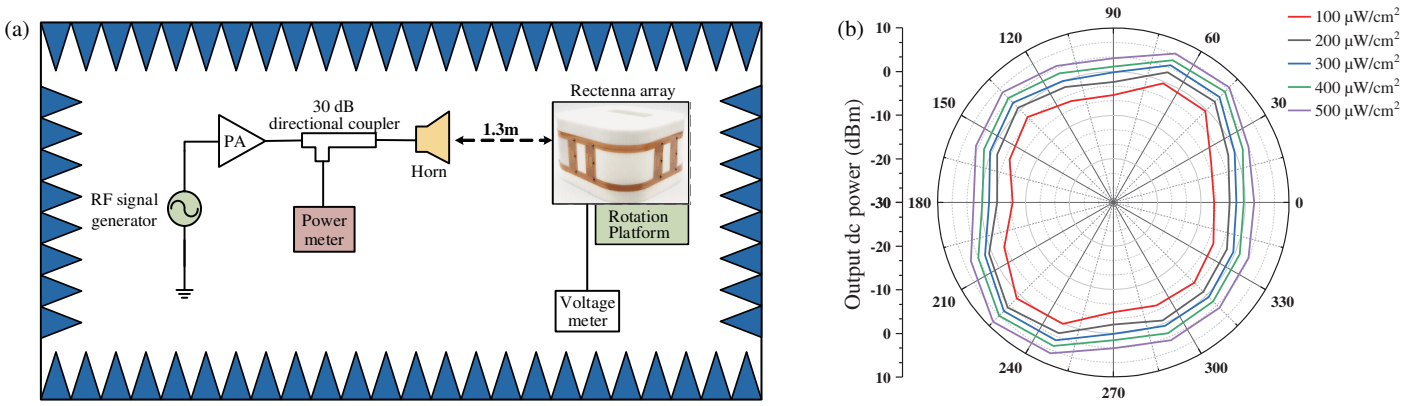

FIGURE 10. Rectenna array measurement. (a) Measurement system. (b) Measurements.

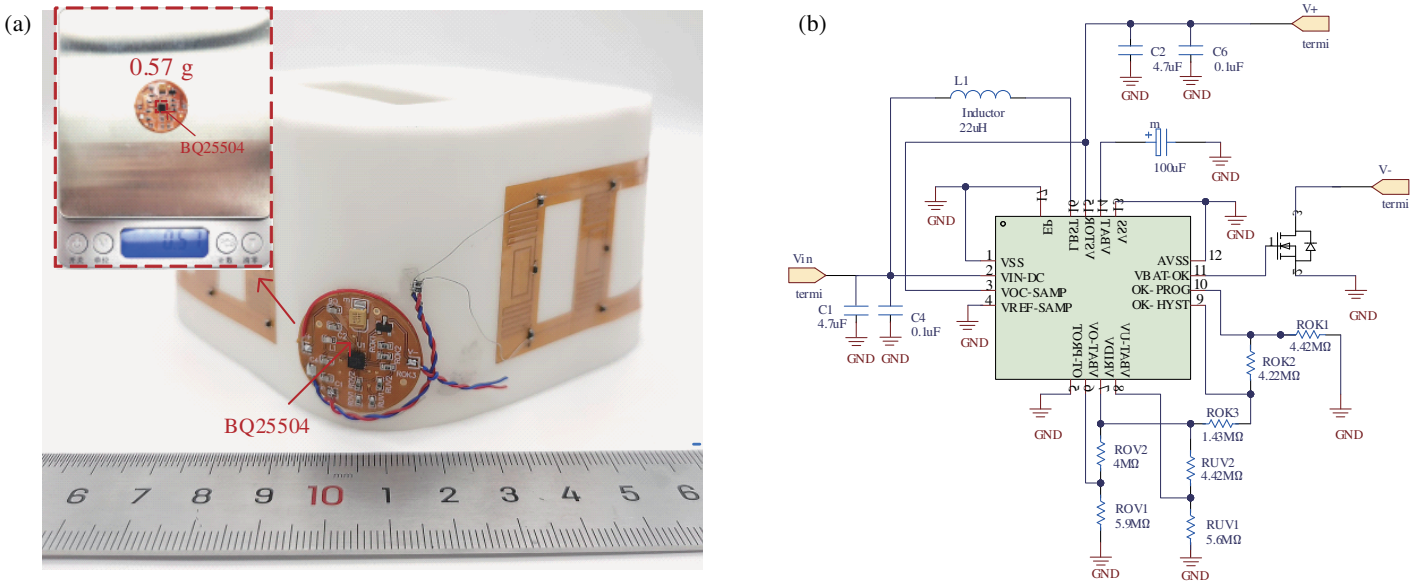

FIGURE 11. BQ25504 energy management circuit. (a) BQ25504 fabrication. (b) BQ25504 schematic.

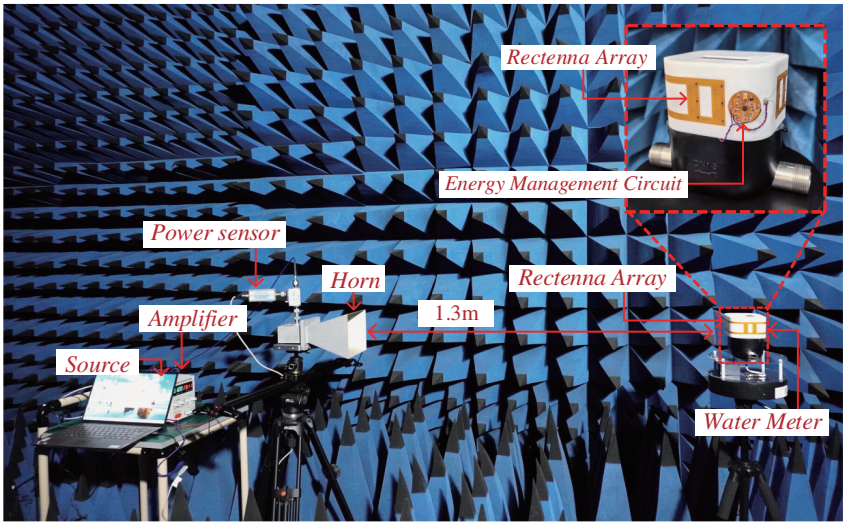

FIGURE 12. The test system of the energy management circuit driving the water meter.

TABLE 3. Comparison of the proposed rectenna array and related designs.

References	Frequency (GHz)	Flexible	Dimensions (mm)	Single element or array	Omnidirectional	Matching network	Efficiency
[20]	0.9–1.1, 1.8–2.5	No	Single element: $130 \times 130 \times 1.52$	1	No	No	Rectenna: 75% @20 dBm
[22]	2.45	Yes	Single element: $88 \times 85 \times 1.5$	2×3 2×2	No	Yes	Rectifier: 35% @-10 dBm
[24]	1.7–1.8, 2.1–2.7	No	Array: $145 \times 145 \times 1.53$	1×12	Yes	No	System: 66% @-3 dBm
[25]	2.45	No	Array: $240 \times 180 \times 1.5$	$3 \times 2 \times 3$	Yes	Yes	Rectifier: 73% @11.3 dBm
This work	2.45	Yes	Single element: $36 \times 11 \times 0.056$	1×8	Yes	No	Rectenna: 65% @6.8 dBm

mm wide metal wires are used to connect those parallel units. The case of the water meter is made of PVC ($\varepsilon r = 2.7$) with a thickness of 1 mm and is non-conductive.

The test system for the rectenna array applied to a water meter is shown in Figure 10(a). At the receiver side, a water meter case affixed with the rectenna array is placed on a rotating platform, and a 100 Ω chip resistor is soldered to the array output as a load. The energy harvesting performance at different angles is measured by rotating the platform.

The power density at the rectenna array is:

$$S_{\text{avg}} = \frac{G_t P_t}{4\pi R^2} \tag{6}$$

where G_t is the dimensionless transmit antenna's gain, P_t the transmitting power in W, and R the distance between the receive and transmit antennas.

The measured output DC power versus the rotation angles in different receiving power densities is shown in Figure 10(b). The output DC power is higher than 0.2 mW (-7 dBm) at different rotation angles when the received power density is 100 μw/cm^2, and the peak output power is 1.3 mW (1.14 dBm). The output DC power is higher than 1.5 mW (1.76 dBm) at different rotation angles when the received power density is 500 μw/cm^2, and the peak output power is 7.4 mW (8.7 dBm). The results show that the water meter with a flexible rectenna array can harvest omnidirectional RF energy. Due to the rotation of the water meter, the main working rectenna units are changed from two to four. The DC power output from the rectenna array reaches the peak at 45°, 135°, 225°, and 315°. When rotating it to 225°, the four main working rectennas are closer to the load, and the system has less energy loss, thus, the output DC power is higher than the other three rotation angles where the peak occurs.

The performance comparison between the proposed rectenna array and related designs is depicted in Table 3. It shows that our design is lightweight and compact while having a flexible structure and omnidirectional energy harvesting. These advantages broaden its applications on IoT devices for environmental energy harvesting.

6. DESIGN AND APPLICATION OF THE ENERGY MANAGEMENT CIRCUIT

The power received by the rectenna during wireless energy harvesting is usually very weak, discontinuous, and unstable, which cannot directly drive the water meter. However, an energy management circuit can store, distribute, and manage the harvested energy. Therefore, it is necessary to introduce an energy management circuit to the output of the rectenna array to provide stable power for the smart water meter.

The schematic and fabrication prototype of the energy management circuit are shown in Figure 11. The energy management circuit is fabricated on a flexible substrate with a mass of only 0.57 g.

The test system of the energy management circuit for the water meter is shown in Figure 12. Measurement results show that the rectenna array can successfully drive the water meter without rotating the water meter when the received power density is 442 μw/cm^2.

7. CONCLUSION

In this manuscript, a conformal flexible omnidirectional rectenna array is designed and implemented for IoT smart water meters. A meander dipole antenna with a coupling loop is designed to directly conjugate match the impedance of the SMS-7630 diode at 2.45 GHz. Each rectenna array unit consists of a meander dipole antenna and an SMS-7630 diode. The flexible polyimide substrate is used to fabricate the rectenna array to conform to the water meter case. A flexible rectenna unit's maximum RF to DC energy conversion efficiency can reach 65%. The flexible rectenna array can output DC power up to 7.4 mW when the received power density is 500 μW/cm^2 and can achieve omnidirectional environmental energy harvesting. The proposed flexible rectenna array is of great research significance for smart water metering applications towards the Internet of Things.

ACKNOWLEDGEMENT

This work was supported in part by the NSFC U22A2015 and 62071316.

REFERENCES

[1] Lin, W. and R. W. Ziolkowski, "Wireless power transfer (WPT) enabled iot sensors based on ultra-thin electrically small antennas," in *2021 15th European Conference on Antennas and Propagation (EUCAP)*, Electr Network, Mar. 2021.

[2] Takamori, R., M. Kawasaki, H. Seita, K. Nishimori, N. Honma, K. Nishikawa, Y. Maru, and S. Kawasaki, "Wireless sensor network in reusable vehicle rocket and low-power 20-30 GHz amplifier MMIC," in *2013 IEEE Wireless Power Transfer (WPT)*, 96–99, Perugia, Italy, May 2013.

[3] Halivni, B. and M. M. Peretz, "Current controlled transmitter for high frequency WPT utilizing non-invasive PCB integrated rogowski current sensor," in *2023 IEEE Applied Power Electronics Conference and Exposition, APEC*, 1639–1644, Orlando, Fl, Mar. 2023.

[4] Salvati, R., V. Palazzi, G. Cicioni, G. Simoncini, F. Alimenti, M. M. Tentzeris, P. Mezzanotte, and L. Roselli, "Zero-power wireless pressure sensor based on backscatterer harmonic transponder in a WPT context," in *2022 Wireless Power Week (WPW)*, 199–202, Bordeaux, France, Jul. 2022.

[5] Lee, G., H. Gwak, Y.-S. Kim, and W.-S. Park, "Wireless power transfer system for diagnostic sensor on rotating spindle," in *2013 IEEE Wireless Power Transfer (WPT)*, 100–102, Perugia, Italy, May 2013.

[6] Zhang, H., Y.-X. Guo, Z. Zhong, and W. Wu, "Cooperative integration of RF energy harvesting and dedicated WPT for wireless sensor networks," *IEEE Microwave and Wireless Components Letters*, Vol. 29, No. 4, 291–293, Apr. 2019.

[7] Shiba, K. and M. Takahashi, "A development of WPT devices for wireless-powered small sensors for home health care," in *2022 International Symposium on Antennas and Propagation (ISAP)*, 81–82, Sydney, Australia, Oct. 2022.

[8] Dande, B., C.-Y. Chang, and C.-D. Fan, "Mobile charger scheduling algorithm for energy recharging in wireless sensor networks," in *2022 International Conference on Electronic Systems and Intelligent Computing (ICESIC)*, 18–22, 2022.

[9] Katbay, Z., D. Sounas, and M. Ismail, "Wireless charging of IOT devices in smart homes using retrodirective WPT," in *2021 IEEE International Midwest Symposium on Circuits and Systems (MWSCAS)*, 962–965, Electr Network, Aug. 2021.

[10] Merabet, A., A. Lakas, and A. N. Belkacem, "WPT-enabled multi-UAV path planning for disaster management deep Q-network," in *2023 International Wireless Communications and Mobile Computing, IWCMC*, 1672–1678, Marrakesh, Morocco, Jun. 2023.

[11] Amith, B., A. S. Kadam, A. Kulkarni, and P. R. Sankpal, "IOT based smart water meter for water management," in *2023 International Conference on Intelligent and Innovative Technologies in Computing, Electrical and Electronics (IITCEE)*, 674–678, 2023.

[12] Ray, A. and S. Goswami, "IOT and cloud computing based smart water metering system," in *2020 International Conference on Power Electronics & IOT Applications in Renewable Energy and Its Control (PARC)*, 308–313, 2020.

[13] Qiao, X., S. Niu, J. Lin, M. Chen, and Y. Wu, "A novel magnetically coupled resonant wireless power transfer technique used in rotary ultrasonic machining process," in *2021 IEEE Wireless Power Transfer Conference (WPTC)*, Electr Network, Jun. 2021.

[14] Dong, Y., S.-W. Dong, S. Gao, Y. Wang, X. Li, and G. Wei, "Design of microwave power transmission system for space solar power station demonstration," in *2020 IEEE Wireless Power Transfer Conference (WPTC)*, 13–15, Electr Network, Nov. 2020.

[15] Liu, C., F. Tan, H. Zhang, and Q. He, "A novel single-diode microwave rectifier with a series band-stop structure," *IEEE Transactions on Microwave Theory and Techniques*, Vol. 65, No. 2, 600–606, Feb. 2017.

[16] Zhang, B., X. Zhao, C. Yu, K. Huang, and C. Liu, "A power enhanced high efficiency 2.45 GHz rectifier based on diode array," *Journal of Electromagnetic Waves and Applications*, Vol. 25, No. 5-6, 765–774, 2011.

[17] He, Z., H. Lin, and C. Liu, "A novel class-C rectifier with high efficiency for wireless power transmission," *IEEE Microwave and Wireless Components Letters*, Vol. 30, No. 12, 1197–1200, Dec. 2020.

[18] He, Z. and C. Liu, "A compact high-efficiency broadband rectifier with a wide dynamic range of input power for energy harvesting," *IEEE Microwave and Wireless Components Letters*, Vol. 30, No. 4, 433–436, Apr. 2020.

[19] He, Z., J. Lan, and C. Liu, "Compact rectifiers with ultra-wide input power range based on nonlinear impedance characteristics of schottky diodes," *IEEE Transactions on Power Electronics*, Vol. 36, No. 7, 7407–7411, Jul. 2021.

[20] Song, C., Y. Huang, J. Zhou, P. Carter, S. Yuan, Q. Xu, and Z. Fei, "Matching network elimination in broadband rectennas for high-efficiency wireless power transfer and energy harvesting," *IEEE Transactions on Industrial Electronics*, Vol. 64, No. 5, 3950–3961, May 2017.

[21] Sun, H., Y.-X. Guo, M. He, and Z. Zhong, "Design of a high-efficiency 2.45-GHz rectenna for low-input-power energy harvesting," *IEEE Antennas and Wireless Propagation Letters*, Vol. 11, 929–932, 2012.

[22] Vital, D., S. Bhardwaj, and J. L. Volakis, "Textile-based large area RF-power harvesting system for wearable applications," *IEEE Transactions on Antennas and Propagation*, Vol. 68, No. 3, 2, 2323–2331, Mar. 2020.

[23] Kim, J., C. Cha, K. Lee, J. Oh, and Y. Hong, "E-textile-based wavy surface WPT flexible antenna with frequency self-reconfiguration function for batteryless sensor platform," *IEEE Sensors Journal*, Vol. 23, No. 5, 4392–4404, Mar. 2023.

[24] Song, C., P. Lu, and S. Shen, "Highly efficient omnidirectional integrated multiband wireless energy harvesters for compact sensor nodes of Internet-of-Things," *IEEE Transactions on Industrial Electronics*, Vol. 68, No. 9, 8128–8140, Sep. 2021.

[25] Sun, H., J. Huang, and Y. Wang, "An omnidirectional rectenna array with an enhanced RF power distributing strategy for RF energy harvesting," *IEEE Transactions on Antennas and Propagation*, Vol. 70, No. 6, 4931–4936, Jun. 2022.